IEEE Access
Multidisciplinary ⋮ Rapid Review ⋮ Open Access Journal

Received March 2, 2021, accepted March 20, 2021, date of publication March 23, 2021, date of current version April 5, 2021.

Digital Object Identifier 10.1109/ACCESS.2021.3068289

Joint Trajectory and Hybrid Beamforming Design for Multi Antenna UAV Enabled Network

FENG ZHOU AND RUGANG WANG
School of Information Technology, Yancheng Institute of Technology, Yancheng 224051, China
Research Center of Photoelectric Technology, Yancheng Institute of Technology, Yancheng 224051, China

Corresponding author: Feng Zhou (zfycit@ycit.edu.cn)

This work was supported in part by the National Natural Science Foundation of China under Grant 61673108, in part by the Colleges and Universities Natural Science Foundation in Jiangsu Province under Contract 19KJA110002, and in part by the Industry-University-Research Cooperation Project of Jiangsu Province under Grant BY2020358 and Grant BY2020335.

ABSTRACT In this paper, we investigate the transmission design in a multi antenna unmanned aerial vehicle (UAV)-enabled network, where the flight trajectory and hybrid digital and analog beamforming (BF) of the UAV are jointly designed, for both the fully-connected structure and sub-connected structure. Our goal is to maximize the weighted sum rate for multiply ground users, subject to the transmit power and trajectory constraints. Due to the non-convex property of the formulated problem, we propose to linearize the objective by using a newly Lagrangian dual transform. Then, an alternating optimization (AO) method is proposed, where the digital BF can be obtained by utilizing the bisection search method, while the analog BF and the flight trajectory are handled by the alternating direction of multipliers method (ADMM) algorithm. Finally, simulation results verify the performance of the proposed algorithm.

INDEX TERMS Hybrid digital and analog beamforming, alternating optimization, alternating direction of multipliers method, trajectory design.

I. INTRODUCTION

Recently, unmanned aerial vehicle (UAV) is treated as an emerging technology which has been widely investigated in military, public, and civil scenarios [1]. Due to advantages such as low-altitude deployment and strong communication links with the ground, UAVs have been widely used in several applications [2]. Unlike the conventional wireless systems with static access points, UAV-enabled wireless communications often require joint consideration of trajectory planning and communication resource allocation, since UAVs are usually energy constrained [3]. Hence, optimize the trajectory and communication resource is of great importance in UAV applications [4].

Specifically, in [5], the authors investigated the joint trajectory and communication design for multi-UAV enabled wireless networks. In [6], the authors studied the multi-UAV deployment for throughput maximization in the presence of co-channel interference. While in [7], the authors investigated the multi-UAV interference coordination by joint trajectory and power control. Furthermore, in [8], the authors investigated the joint cache placement, flight trajectory, and power control for UAV assisted wireless networks. In addition, in [9], the authors studied the optimal three dimensional trajectory design and resource allocation for solar-powered UAV communication systems, where a mixed-integer non-convex optimization problem was proposed, taking into account the aerodynamic power consumption, the solar energy harvesting, the finite energy storage capacity, and the quality-of-service (QoS) requirements of the users. Also, energy efficient UAV communication have been investigated in [10] and [11], where the Dinkebach method was commonly used to transform the fractional programming to a linear optimization, but the computational complexity is high. Recently, in [12], the authors investigated the trajectory and transmit power optimization in secrecy UAV communication network, and was extended in [13] with considering robust design to handle the uncertainty ground user locations.

However, these works focus on the single antenna UAV case. In fact, large scale multiple antenna technique has attracted considerable interest for the development of the next generation wireless networks, since it can dramatically increase the system capacity and mitigate the spectrum shortage [14]. Recently, the multiple antenna technique enabled UAV communication has been investigated in several works

The associate editor coordinating the review of this manuscript and approving it for publication was Amjad Mehmood.

This work is licensed under a Creative Commons Attribution 4.0 License. For more information, see https://creativecommons.org/licenses/by/4.0/

such as [15]–[17]. For instance, in [15], the authors studied the robust trajectory and resource allocation design in multiple antenna UAV networks. While in [16], the authors investigated the joint trajectory and resource allocation design for energy-efficient secure multiple antenna UAV communication system. Also in [17], the authors studied the energy-efficient and secure multiple antenna UAV communication with jittering. Nevertheless, the conventional fully digital beamforming (BF) structure imposes an excessive fabrication cost and energy consumption owing to using numerous costly radio frequency (RF) chains and analog-digital (A/D) converters.

To overcome this obstacle, the newly hybrid A/D BF technique has been proposed as a promising way, which relies on a lower number of RF chains than the fully digital BF method [18]. However, the main challenges in the design of hybrid BF arise from the transmit power constraint with coupling components, imposed by the product of digital and analog BF matrices, and by the unit modulus constraint (UMC) on the elements of the analog BF matrix [19].

To solve this problem, several methods were proposed in related literatures. Specifically, in [20], the authors proposed a matrix factorization method to obtain the hybrid BF matrices based on the Broyden-Fletcher-Goldfarb-Shanno (BFGS) algorithm. While in [21], the digital BF was derived according to the original objective, while the analog BF was handled by several iterative algorithms. Also in [22], the authors investigated the hybrid BF design based on a joint iterative algorithm. In [23], secure communication for spatially sparse multiple-input multiple-output (MIMO) channel with hybrid precoding was proposed. What's more, in [24], the authors investigated the hybrid precoding using deep learning method for MIMO network. Recently in [25], the authors proposed a hybrid BF method in multiple-input single-output (MISO) wiretap channel to improve the security.

Due to the limited power, volume and cost, it may be impractical to equipment many RF links in a UAV [26]. Thus, the hybrid BF technique is a promising way to improve the spectrum efficiency in a multi antenna UAV-enabled network. However, such work has not been studied yet. Besides, the trajectory optimization method in related work mainly based on the successive convex approximation (SCA) and inner point method, which may lead to high computational complexity, thus is hard to conduct on the UAV. Motivated by this, this paper investigates a new paradise of the transmission in a multi antenna UAV network, where the UAV provide service for multiple ground users. Specifically, we aim to maximize the weighted sum rate (WSR) by jointly designing the hybrid BF and flight trajectory of the UAV, where both the fully-connected structure and sub-connected structure are considered. To solve the formulated non-convex problem, we propose to linearize the objective by a newly Lagrangian dual transform. Then, an alternating optimization (AO) method is proposed to obtain the solution, where the analog BF matrix and the trajectory are handled by the alternating direction of multipliers method (ADMM) technique. Finally, simulation results are provided to verify the proposed algorithm.

We summarize our main contributions as follows:

- To the best of our knowledge, similar work about exploiting the hybrid BF in UAV communication network to improve the spectrum efficiency has not been investigated yet. The formulated WSR maximization design is non-convex, due to the complex objective and multiple coupled variables. Since it is difficult to obtain the globally optimal solution, we propose an AO algorithm to obtain a suboptimal solution, where each subproblem can be solved efficiently and the variables are alternately optimized in an iterative manner until convergence.
- By a newly Lagrangian dual transform, we transform the original problem into a quadratic form, which is beneficial for optimization. Specifically, the bisection search method is proposed to design the digital BF matrix. Then, an ADMM method is proposed to handle the UMC of the analog BF matrix, which is suitable for both the fully connected case and the sub connected case. While for the trajectory design, by decoupling the maximum speed constraints into a linear constraint, a low complexity ADMM method is proposed.
- The computational complexity and the convergence of the AO method are analyzed. In fact, the proposed method has lower complexity than the interior-point method, which is beneficial for implementation online and onboard on the UAV. Besides, simulation results suggest that the proposed algorithm can apparently improve the spectrum efficiency, when compared to other benchmark schemes such as the no trajectory design or the random BF method.

The rest of this paper is organized as follows. A system model and problem statement is given in Section II. Section III investigates the joint design problem, wherein a Lagrangian dual transform based method is proposed. Simulation results are illustrated in Section IV. Section V concludes this paper.

Notations: Throughout this paper, the upper case boldface letters and lower case boldface letters are used to denote matrices and vectors, respectively. $\mathbf{A}^H$, $\mathbf{A}^T$, $\mathbf{A}^\dagger$, $\mathrm{Tr}(\mathbf{A})$ and $\mathrm{vec}(\mathbf{A})$ denote the Hermitian transpose, the transpose, the conjugate, the trace and the vectorization of matrix $\mathbf{A}$, respectively. $\|\cdot\|$ denotes the Euclidean norm of a vector, or the Frobenius norm of a matrix. $\Re\{a\}$ and $|a|$ denote the real part and the modulus of a complex a, respectively. $\mathbf{x} \sim \mathcal{CN}(\mathbf{u}, \Omega)$ denotes that $\mathbf{x}$ is a circularly symmetric complex Gaussian (CSCG) random vector with mean $\mathbf{u}$ and covariance Ω. $\star$ denotes the optimal value of a variable.

II. SYSTEM MODEL AND PROBLEM STATEMENT

A. SYSTEM MODEL

Let us consider a UAV-enabled communication system as shown in Fig. 1, which consists of a UAV and multiply

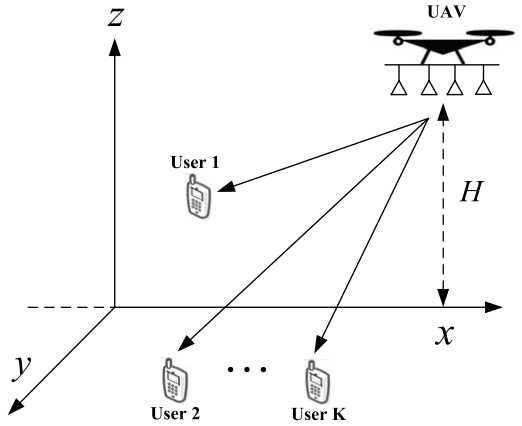

FIGURE 1. System model for multi antenna UAV-aided multiuser network.

single antenna ground users. The UAV is equipped with N_t antennas and N_{RF} RF links. Without loss of generality, we consider a three-dimensional (3D) Cartesian coordinate system. The coordinate of the k-th user is denoted as $\mathbf{q}_k = [x_k, y_k]^T$. The UAV is assumed to fly horizontally at a constant altitude H in m from the pre-determined initial location $\mathbf{q}_0 = [x_0, y_0]^T$, to the final location $\mathbf{q}_f = [x_f, y_f]^T$, in a finite time T. T is divided into N time slots with each slot duration $\delta_T = T/N$, which is small enough such that the location of the UAV can be seen as a constant within each time slot, and the horizontal coordinate of the UAV in slot n is $\mathbf{q}[n] = [x[n], y[n]]^T, n = 1, \cdots, N$.

Subject to the maximum speed constraints, the UAV trajectory should satisfy the following conditions [2]

$$\|\mathbf{q}[1] - \mathbf{q}_0\|^2 \leq S_{max}^2, \tag{1a}$$

$$\|\mathbf{q}[n+1] - \mathbf{q}[n]\|^2 \leq S_{max}^2, \quad n = 1, \ldots, N-1, \tag{1b}$$

$$\|\mathbf{q}_f - \mathbf{q}[N]\|^2 \leq S_{max}^2, \tag{1c}$$

where $S_{\max} = V_{\max}\delta_T$ is the maximum distance that the UAV can fly within one slot on the assumption of maximum speed $V_{\max}$ in meter/second (m/s).

The analog precoding matrices map the signals from the RF chains to the transmit antennas using the phase shifting networks. Therefore, every phase shifter in the network should satisfy the UMC, which is translated as a constraint on each entry of the analog precoding matrices, that is, $|\mathbf{F}_{u,v}| = 1, \forall u \in N_t, \forall v \in N_{RF}$. We consider the two most common hybrid architectures namely, e.g., the fully-connected and sub-connected ones, which are shown in Fig. 2 and Fig. 3, respectively. In the former case, the signal from each RF chain is connected to all the antennas via the phase shifting network, whereas in latter, the signal from each RF chain is connected to a subset of antennas. The total number of phase shifters required to implement a fully-connected architecture on the transmitter sides is $N_t \times N_{RF}$. On the other hand, for the sub-connected architecture, each RF chain is connected to N_t/N_{RF} antennas on the transmitter,

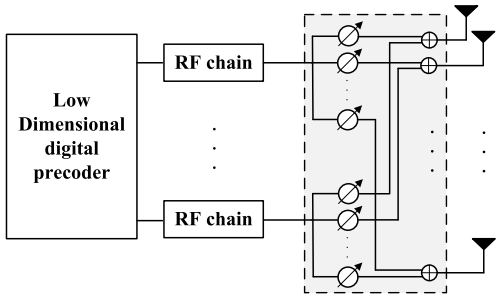

FIGURE 2. The fully-connected architecture.

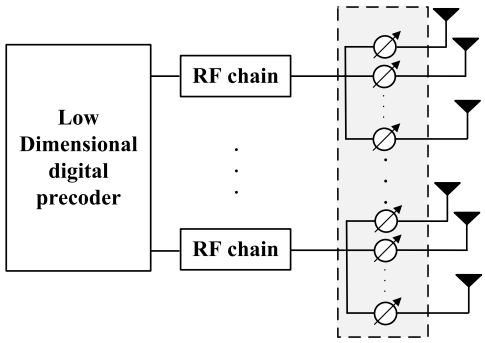

FIGURE 3. The sub-connected architecture.

as shown below,

$$\mathbf{F} = \begin{bmatrix} \mathbf{f}_1 & \mathbf{0} & \cdots & \mathbf{0} \\ \mathbf{0} & \mathbf{f}_2 & \cdots & \mathbf{0} \\ \vdots & \vdots & \ddots & \mathbf{0} \\ \mathbf{0} & \mathbf{0} & \cdots & \mathbf{f}_{N_{RF}} \end{bmatrix}, \tag{2}$$

where each $\mathbf{f}_i$ is $N_t/N_{RF} \times 1$ dimensional vector consisting unit modulus entries [29]. Thus, this architecture requires fewer phase shifters compared to the fully-connected architecture, but at the expense of loss in spectrum efficiency.

The transmit signal by the UAV in the n-th slot can be expressed as [18]

$$x[n] = \sum_{i=1}^{K} \mathbf{F}[n]\mathbf{w}_i[n]s_i[n], \tag{3}$$

where $\mathbf{F}[n] \in \mathbb{C}^{N_t \times N_{RF}}$ denotes the analog BF matrix, $\mathbf{w}_i[n] \in \mathbb{C}^{N_{RF} \times 1}$ and $s_i[n]$ denote the digital BF vector and the intended signal for the i-th user at the n-th slot, respectively.

In this paper, we assume that the air-to-ground communication links between the UAV and the ground users are line-of-sight (LoS) channels, as [12] and [15]. In fact, it is shown that for the rural macro with UAV and urban macro with UAV scenarios, if the UAV height is larger than 40 m and 100 m, respectively, the LoS probability is almost 100% [27]. In particular, the channel vector between the UAV and the k-th user in time slot n is given by [13]

$$\mathbf{h}_k[n] = \sqrt{\rho}\Big(\|\mathbf{q}[n] - \mathbf{q}_k\|^2 + H^2\Big)^{-\frac{1}{2}}\mathbf{a}_k[n], \tag{4}$$

where $\rho = \left(\frac{\lambda_c}{4\pi}\right)^2$ is a constant with λ_c being the wavelength of the center frequency of the carrier [28]. Moreover, $\mathbf{a}_k[n]$ is

the antenna array response (AAR) between the UAV and user k in time slot n. For the AAR, when the uniform linear arrays (ULA) is utilized by the UAV, then, $\mathbf{a}_k[n]$ is given by

$$\mathbf{a}_k[n]=\left[1, e^{-j2\pi \frac{b}{\lambda_c}\cos\varphi_k \sin\theta_k}, \ldots, e^{-j2\pi \frac{b}{\lambda_c}(N_t-1)\cos\varphi_k \sin\theta_k}\right]^T, \tag{5}$$

where φ_k and θ_k (in rads) are the azimuth and elevation angles of departure (AoD) of the path between the ULA and the k-th user in the n-th slot, respectively. In addition, b is the antenna spacing of the ULA [28]. It should be noted that in this work, the jittering of the UAV is neglected since we assume that the AoD is mainly determined by the locations of the UAV and the users. Besides, for some other UAV-ground channel models such as the altitude dependent model [17], the proposed hybrid BF method can still work.

Thus, the received signal by the k-th user in the n-th slot can be expressed as [15]

$$\begin{aligned} y_k[n] &= \mathbf{h}_k[n]\mathbf{F}[n]\mathbf{w}_k[n]s_k[n] \\ &\quad +\mathbf{h}_k[n]\sum_{i\neq k}^{K}\mathbf{F}[n]\mathbf{w}_i[n]s_i[n]+z_k[n], \end{aligned} \tag{6}$$

where $z_k[n]\sim\mathcal{CN}\left(0,\sigma_k^2[n]\right)$ is the additive white Gaussian noise (AWGN).

The signal-to-interference-and-noise-ratio (SINR) for the k-th user at the n-th slot is [15]

$$\begin{aligned} &\gamma_k[n] \\ &= \frac{\frac{\xi_0}{H^2+\|\mathbf{q}[n]-\mathbf{q}_k\|^2}\left|\mathbf{h}_k^H[n]\mathbf{F}[n]\mathbf{w}_k[n]\right|^2}{\frac{\xi_0}{H^2+\|\mathbf{q}[n]-\mathbf{q}_k\|^2}\sum\limits_{i=1,i\neq k}^{K}\left|\mathbf{h}_k^H[n]\mathbf{F}[n]\mathbf{w}_i[n]\right|^2+\sigma_k^2} \\ &= \frac{\left|\mathbf{h}_k^H[n]\mathbf{F}[n]\mathbf{w}_k[n]\right|^2}{\sum\limits_{i=1,i\neq k}^{K}\left|\mathbf{h}_k^H[n]\mathbf{F}[n]\mathbf{w}_i[n]\right|^2+\tilde{\sigma}_k^2\left(H^2+\|\mathbf{q}[n]-\mathbf{q}_k\|^2\right)}, \end{aligned} \tag{7}$$

where $\tilde{\sigma}_k^2=\sigma_k^2/\xi_0$.

B. PROBLEM STATEMENT

In this work, we investigate the average WSR maximization problem by jointly designing the hybrid BF and flight trajectory. Mathematically, the problem is given by

$$\max_{\mathbf{W}[n],\mathbf{F}[n],\mathbf{q}[n]} \ \frac{1}{N}\sum_{n=1}^{N}\sum_{k=1}^{K}\omega_k[n]\log_2\left(1+\gamma_k[n]\right) \tag{8a}$$

$$\text{s.t.} \ \sum_{n=1}^{N}\|\mathbf{F}[n]\mathbf{w}_k[n]\|^2\leq N\bar{P},\ \|\mathbf{F}[n]\mathbf{w}_k[n]\|^2\leq\hat{P}, \quad \forall k,\ \forall n, \tag{8b}$$

$$\left|\mathbf{F}_{u,v}\right|=1, \quad \forall u,v, \tag{8c}$$

where $\mathbf{W}[n]\triangleq[\mathbf{w}_1[n],\ldots,\mathbf{w}_K[n]]\in\mathbb{C}^{N_{RF}\times K}$, $\omega_k[n]\left(0\leq\omega_k[n]\leq 1,\ \sum\limits_{k=1}^{K}\omega_k[n]=1\right)$ denotes the weighted factor for the k-th user at the n-th slot, $\bar{P}$ and $\hat{P}$ denote the average power and the peak power, respectively. In addition, (8c) is the UMC for the analog BF matrix, which is the main difference for the hybrid BF design with the fully digital BF design. In order to simplify the symbolic expression, in the following, we will neglect the slot index n in the associated variables.

III. THE JOINT BF AND TRAJECTORY DESIGN

A. THE LAGRANGIAN DUAL TRANSFORMATION

(8) is hard to solve due to the non-convex objective and constraints [30]. In this section, we will propose an effective way to handle (8).

Firstly, via the Lagrangian dual transform proposed in [31], (8) can be equivalently rewritten as

$$\begin{aligned} \max_{\mathbf{W},\mathbf{F},\mathbf{q},\alpha} \ &\sum_{n=1}^{N}\left\{\sum_{k=1}^{K}\omega_k\log_2\left(1+\alpha_k\right)\right. \\ &\left.-\sum_{k=1}^{K}\omega_k\alpha_k+\sum_{k=1}^{K}\frac{\omega_k\left(1+\alpha_k\right)\gamma_k}{1+\gamma_k}\right\} \end{aligned} \tag{9a}$$

$$\text{s.t.} \ \ (8b), \tag{9b}$$

where $\boldsymbol{\alpha}\triangleq[\alpha_1,\ldots,\alpha_K]^T$, with α_k is the auxiliary variable for the decoding SINR γ_k.

According to [31], in (9), when $\{\mathbf{W},\mathbf{F},\mathbf{q}\}$ hold fixed, the optimal α_k is $\alpha_k^\star=\gamma_k$.

Then, for fixed $\boldsymbol{\alpha}$, (9) is reduced to

$$\max \sum_{n=1}^{N}\sum_{k=1}^{K}\frac{\tilde{\alpha}_k\gamma_k}{1+\gamma_k} \tag{10a}$$

$$\text{s.t.} \ \ (8b), \tag{10b}$$

where $\tilde{\alpha}_k=\omega_k\left(1+\alpha_k\right)$. More details can refer [31].

(10) is the sum of multiple-ratio fractional programming problems, while the non-convexity introduced by the ratio operation can be solved by the recently proposed technique in [32]. Then, (10) can be solved in an AO method. In particular, in each iteration, we first update the SINR $\boldsymbol{\alpha}$, and then update $\{\mathbf{W},\mathbf{F},\mathbf{q}\}$, respectively. The process is repeated until no further improvement is obtained.

Specifically, using γ_k in (7), the objective function of (10) is rewritten as

$$\begin{aligned} &f_1(\mathbf{W},\mathbf{F},\mathbf{q}) \\ &= \sum_{n=1}^{N}\sum_{k=1}^{K}\frac{\tilde{\alpha}_k\gamma_k}{1+\gamma_k} \\ &= \sum_{n=1}^{N}\sum_{k=1}^{K}\frac{\tilde{\alpha}_k\left|\mathbf{h}_k^H\mathbf{F}\mathbf{w}_k\right|^2}{\sum\limits_{i=1}^{K}\left|\mathbf{h}_k^H\mathbf{F}\mathbf{w}_i\right|^2+\tilde{\sigma}_k^2\left(H^2+\|\mathbf{q}-\mathbf{q}_k\|^2\right)}. \end{aligned} \tag{11}$$

Thus, with given $\boldsymbol{\alpha}$, (9) becomes

$$\max_{\mathbf{W},\mathbf{F},\mathbf{q}} \ \ f_1(\mathbf{W},\mathbf{F},\mathbf{q}) \tag{12a}$$

$$\text{s.t.} \ \ (8b). \tag{12b}$$

It is known that (12) is a multiple-ratio fractional programming (FP) problem. Using the quadratic transform proposed in [32], $f_1(\mathbf{W}, \mathbf{F}, \mathbf{q})$ can be equivalently reformulated as

$$\begin{aligned} &f_2(\mathbf{W}, \mathbf{F}, \mathbf{q}, \boldsymbol{\beta}) \\ &= \sum_{n=1}^{N}\sum_{k=1}^{K} 2\sqrt{\tilde{\alpha}_k}\Re\left\{\beta_k^{\dagger}\mathbf{h}_k^H\mathbf{F}\mathbf{w}_k\right\} \\ &\quad - \sum_{n=1}^{N}\sum_{k=1}^{K}|\beta_k|^2\left(\sum_{i=1}^{K}\left|\mathbf{h}_k^H\mathbf{F}\mathbf{w}_i\right|^2 + \tilde{\sigma}_k^2\left(H^2 + \|\mathbf{q}-\mathbf{q}_k\|^2\right)\right), \end{aligned} \tag{13}$$

where $\boldsymbol{\beta} \triangleq [\beta_1, \ldots, \beta_K]^T$, with $\beta_k \in \mathbb{C}$ is the auxiliary variable. Then, based on [32], solving (13) over $\{\mathbf{W}, \mathbf{F}, \mathbf{q}\}$ is equivalent to solving the following problem with respect to (w.r.t.) $\{\mathbf{W}, \mathbf{F}, \mathbf{q}, \boldsymbol{\beta}\}$

$$\max_{\mathbf{W},\mathbf{F},\mathbf{q},\boldsymbol{\beta}} \quad f_2(\mathbf{W}, \mathbf{F}, \mathbf{q}, \boldsymbol{\beta}) \tag{14a}$$

$$\text{s.t.} \quad (8b). \tag{14b}$$

(14) is a biconvex optimization problem, and a common method for solving it is alternatively updating $\{\mathbf{W}, \mathbf{F}, \mathbf{q}, \boldsymbol{\beta}\}$ by optimizing one of them while fixing the other variables [33]. First, we introduce the following Theorem.

Theorem 1: With given $\{\mathbf{W}, \mathbf{F}, \mathbf{q}\}$, the optimal β_k is

$$\beta_k^{\star} = \frac{\sqrt{\tilde{\alpha}_k}\mathbf{h}_k^H\mathbf{F}\mathbf{w}_k}{\sum_{i=1}^{K}\left|\mathbf{h}_k^H\mathbf{F}\mathbf{w}_i\right|^2 + \tilde{\sigma}_k^2\left(H^2 + \|\mathbf{q}-\mathbf{q}_k\|^2\right)}. \tag{15}$$

Proof: $\beta_k^{\star}$ can be obtained by setting $\partial f_2 / \partial \beta_k$ to zero.

B. THE HYBRID BF DESIGN

In this subsection, we will investigate the hybrid BF design.

1) THE DIGITAL BF DESIGN

Firstly, we solve the digital BF design. By fixing $\{\mathbf{F}, \mathbf{q}, \boldsymbol{\beta}\}$, the subproblem w.r.t. $\mathbf{w}_k$ is given by

$$\begin{aligned} \max_{\mathbf{w}_k} \sum_{n=1}^{N}\Bigg\{&\sum_{k=1}^{K} 2\sqrt{\tilde{\alpha}_k}\Re\left\{\beta_k^{\dagger}\mathbf{h}_k^H\mathbf{F}\mathbf{w}_k\right\} \\ &- \sum_{k=1}^{K}|\beta_k|^2\sum_{i=1}^{K}\left|\mathbf{h}_k^H\mathbf{F}\mathbf{w}_i\right|^2\Bigg\} \end{aligned} \tag{16a}$$

$$\text{s.t.} \quad (8b). \tag{16b}$$

For (16), the optimal $\mathbf{w}_k$ is

$$\mathbf{w}_k^{\star} = \sqrt{\tilde{\alpha}_k}\beta_k\left(\lambda\mathbf{F}^H\mathbf{F} + \sum_{i=1}^{K}|\beta_i|^2\mathbf{F}^H\mathbf{h}_i\mathbf{h}_i^H\mathbf{F}\right)^{-1}\mathbf{F}^H\mathbf{h}_k, \tag{17}$$

where λ is the dual variable introduced for the power constraint, which is determined by

$$\lambda^{\star} = \min\left\{\lambda \geq 0 : \sum_{k=1}^{K}\|\mathbf{F}\mathbf{w}_k\|^2 \leq P_s\right\}, \tag{18}$$

and can be obtained by the bisection search method.

2) THE ANALOG BF DESIGN

In this subsection, we propose the ADMM method to optimize the analog BF $\mathbf{F}$ with fixed $\{\mathbf{W}, \mathbf{q}, \boldsymbol{\beta}\}$. Specifically, the subproblem w.r.t. $\mathbf{F}$ is given by

$$\begin{aligned} \max_{\mathbf{F}} \sum_{n=1}^{N}\Bigg\{&\sum_{k=1}^{K} 2\sqrt{\tilde{\alpha}_k}\Re\left\{\beta_k^{\dagger}\mathbf{h}_k^H\mathbf{F}\mathbf{w}_k\right\} \\ &- \sum_{k=1}^{K}|\beta_k|^2\sum_{i=1}^{K}\left|\mathbf{h}_k^H\mathbf{F}\mathbf{w}_i\right|^2\Bigg\} \end{aligned} \tag{19a}$$

$$\text{s.t.} \quad (8c). \tag{19b}$$

In fact, the only non-convexity in (19) is the UMC (8c). To handle this, we introduce the auxiliary variables $\mathbf{Q}$ and convert (19) into the following problem

$$\begin{aligned} \max_{\mathbf{F},\mathbf{Q}} \sum_{n=1}^{N}\Bigg\{&\sum_{k=1}^{K} 2\sqrt{\tilde{\alpha}_k}\Re\left\{\beta_k^{\dagger}\mathbf{h}_k^H\mathbf{F}\mathbf{w}_k\right\} \\ &- \sum_{k=1}^{K}|\beta_k|^2\sum_{i=1}^{K}\left|\mathbf{h}_k^H\mathbf{F}\mathbf{w}_i\right|^2\Bigg\} \end{aligned} \tag{20a}$$

$$\text{s.t.} \quad \mathbf{F} = \mathbf{Q}, \tag{20b}$$

$$\left|\mathbf{Q}_{u,v}\right| = 1, \forall u, v. \tag{20c}$$

The augmented Lagrangian function of (20) is given by

$$\begin{aligned} \mathcal{L}(\mathbf{F}, \mathbf{Q}, \mathbf{P}) = \sum_{n=1}^{N}\Bigg\{&\sum_{i=1}^{K} -2\sqrt{\tilde{\alpha}_k}\Re\left\{\beta_k^{\dagger}\mathbf{h}_k^H\mathbf{F}\mathbf{w}_k\right\} \\ &+ \sum_{k=1}^{K}|\beta_k|^2\sum_{i=1}^{K}\left|\mathbf{h}_k^H\mathbf{F}\mathbf{w}_i\right|^2\Bigg\} - \sum_{n=1}^{N}\langle\mathbf{P}, \mathbf{F}-\mathbf{Q}\rangle \\ &+ \frac{\rho_0}{2}\sum_{n=1}^{N}\|\mathbf{F}-\mathbf{Q}\|^2, \end{aligned} \tag{21}$$

where $\rho_0 \geq 0$ is the scalar penalty factor, and $\mathbf{P} \in \mathbb{C}^{N_t \times N_{RF}}$ is the Lagrangian multiplier matrix associated with (20b). In addition, $\langle\mathbf{A}, \mathbf{B}\rangle = \sum_{u,v}\mathbf{A}_{u,v}^{\dagger}\mathbf{B}_{u,v}$ for matrices $\mathbf{A}$ and $\mathbf{B}$.

Then, the following iterative steps derives from (21) are applied to solve (20)

$$\mathbf{F}^{m+1} = \arg\min_{\mathbf{F}} \ \mathcal{L}\left(\mathbf{F}^m, \mathbf{Q}^m, \mathbf{P}^m\right), \tag{22a}$$

$$\mathbf{Q}^{m+1} = \arg\min_{|\mathbf{Q}_{u,v}|=1,\forall u,v} \ \mathcal{L}\left(\mathbf{F}^{m+1}, \mathbf{Q}^{m+1}, \mathbf{P}^m\right), \tag{22b}$$

$$\mathbf{P}^{m+1} = \mathbf{P}^m - \rho_0\left(\mathbf{F}^{m+1} - \mathbf{Q}^{m+1}\right), \tag{22c}$$

for $m = 1, \ldots$ until certain stop criterion is meet.

The main merit of the ADMM method is that each subproblem has closed-form solution. Firstly, via the following relationship

$$\text{Tr}(\mathbf{AB}) = \text{vec}\left(\mathbf{A}^H\right)^H\text{vec}(\mathbf{B}), \tag{23a}$$

$$\text{Tr}\left(\mathbf{A}^H\mathbf{BCD}\right) = \text{vec}(\mathbf{A})^H\left(\mathbf{D}^T \otimes \mathbf{B}\right)\text{vec}(\mathbf{C}), \tag{23b}$$

(22a) can be equivalently rewritten as

$$\mathbf{f}^{m+1} = \arg\min_{\mathbf{f}} \ \mathbf{f}^H \Xi \mathbf{f} - 2\Re\{\boldsymbol{\varpi}\mathbf{f}\} - \mathbf{p}^\dagger \mathbf{f} + \frac{\rho_0}{2}\|\mathbf{f} - \mathbf{q}\|^2 \tag{24}$$

where $\Xi = \left(\sum_{i=1}^{K} \mathbf{w}_i \mathbf{w}_i^H\right)^T \otimes |\beta_k|^2 \mathbf{h}_k \mathbf{h}_k^H$, $\boldsymbol{\varpi} = \text{vec}\left(\left(\sqrt{\tilde{\alpha}_k}\mathbf{w}_k \beta_k^\dagger \mathbf{h}_k^H\right)^H\right)$, and $\{\mathbf{f}, \mathbf{p}, \mathbf{q}\}$ are the vectorizations of $\{\mathbf{F}, \mathbf{P}, \mathbf{Q}\}$.

Via the first order optimization condition, the optimal $\mathbf{f}^{m+1}$ is given by

$$\mathbf{f}^{m+1} = -(\rho_0 + 2\Xi)^{-1}\left(2\boldsymbol{\varpi} + \mathbf{p}^\dagger + \rho_0 \mathbf{q}\right) \tag{25}$$

On the other hand, (22b) is equivalent to

$$\min_{|\mathbf{Q}_{u,v}|=1, \quad \forall u,v} \left\|\mathbf{Q} - \left(\mathbf{F}^{m+1} - \rho_0^{-1}\mathbf{P}^m\right)\right\|^2, \tag{26}$$

and the optimal $\mathbf{Q}^{m+1}$ is

$$\mathbf{Q}_{u,v}^{m+1} = \begin{cases} \dfrac{\left(\mathbf{F}^{m+1} - \rho_0^{-1}\mathbf{P}^m\right)_{u,v}}{\left|\left(\mathbf{F}^{m+1} - \rho_0^{-1}\mathbf{P}^m\right)_{u,v}\right|}, \\ \text{if } \left|\left(\mathbf{F}^{m+1} - \rho_0^{-1}\mathbf{P}^m\right)_{u,v}\right| \neq 0, \\ \mathbf{Q}_{u,v}^m, \text{otherwise.} \end{cases} \tag{27}$$

To this end, we have obtained the optimal hybrid BF for the fully-connected structure. In the following, we will handle the sub-connected design. In fact, the proposed ADMM method can be used to the sub-connected case with some improvement. Specifically, the augmented Lagrangian function is

$$\begin{aligned} &\mathcal{L}(\mathbf{F}, \mathbf{Q}, \mathbf{P}) \\ &= \sum_{n=1}^{N}\left\{\sum_{k=1}^{K} -2\sqrt{\tilde{\alpha}_k}\Re\left\{\beta_k^\dagger \mathbf{h}_k^H \mathbf{F}\mathbf{w}_k\right\}\right. \\ &\quad \left. + \sum_{k=1}^{K}|\beta_k|^2 \sum_{i=1}^{K}\left|\mathbf{h}_k^H \mathbf{F}\mathbf{w}_i\right|^2\right\} \\ &\quad - \sum_{n=1}^{N}\langle \mathbf{P}, \mathbf{F} - \mathbf{Q}\rangle + \sum_{n=1}^{N}\frac{\rho_0}{2}\|\mathbf{F} - \mathbf{Q}\|^2 + \sum_{n=1}^{N}\mathbb{I}_{\mathcal{F}}\{\mathbf{Q}\}, \end{aligned} \tag{28}$$

where the indicator function of an arbitrary set $\mathbb{I}_{\mathcal{F}}\{\mathbf{Q}\}$ is defined as

$$\mathbb{I}_{\mathcal{F}}\{\mathbf{Q}\} = \begin{cases} 0, & \text{if } \mathbf{Q} \in \mathcal{F}, \\ \infty, & \text{if } \mathbf{Q} \notin \mathcal{F}, \end{cases} \tag{29}$$

and $\mathcal{F}$ denotes the sub-connected matrix constraint as shown in (2).

We now proceed to derive the solution of for the sub-connected architecture. Firstly, the subproblem w.r.t. $\mathbf{Q}$ is written in the following compact form

$$\mathbf{Q}^{m+1} = \arg\min_{|\mathbf{Q}_{u,v}|=1} \sum_{n=1}^{N}\frac{\rho_0}{2}\left\|\mathbf{F} - \rho_0^{-1}\mathbf{P} - \mathbf{Q}\right\|^2 + \sum_{n=1}^{N}\mathbb{I}_{\mathcal{F}}\{\mathbf{Q}\}. \tag{30}$$

By exploiting the block diagonal structure of $\mathbf{Q}$, (30) can be further rewritten as

$$\begin{aligned} &\mathbf{Q}[n]_{u,v}^{m+1} \\ &= \arg\min_{\{\phi_u\}_{u=1}^{N_T}} \left\|\mathbf{F}[n](u,;) - \rho_0^{-1}\mathbf{P}[n](u,;) - e^{j\phi_u}\mathbf{I}(v,:)\right\|^2, \end{aligned} \tag{31}$$

where $1 \leq u \leq N_T$, $v = \left\lceil u\frac{N_{RF}}{N_T}\right\rceil$ and $\mathbf{A}(u,;)$ is the u-th row of a matrix $\mathbf{A}$.

(31) is actually a vector approximation under phase rotation problem [34], which solution is given by

$$\begin{aligned} &\mathbf{Q}[n]_{u,v}^{m+1} \\ &= \Pi_{\mathcal{F}}\left\{\left[\mathbf{F}[n]^{m+1}(u,;) - \rho_0^{-1}\mathbf{P}[n]^m(u,;)\right]\mathbf{I}(v,:)^H\right\}, \end{aligned} \tag{32}$$

where $\Pi_{\mathcal{F}}$ is the projection onto the set of $\mathcal{F}$ for an arbitrary matrix $\mathbf{A}$, which is given by

$$\left(\mathbf{A}_{u,v}\right)_{\mathcal{F}} = \begin{cases} 0, \mathbf{A}_{u,v} = 0, \\ \dfrac{\mathbf{A}_{u,v}}{|\mathbf{A}_{u,v}|}, \mathbf{A}_{u,v} \neq 0. \end{cases} \tag{33}$$

The remain step to update $\mathbf{F}$ and $\mathbf{P}$ are the same with the fully-connected case, thus we omit the detail for brevity.

To this end, the ADMM algorithm to obtain $\mathbf{F}$ is summarized in Algorithm 1. In addition, when the penalty parameter ρ_0 satisfies: $\rho_0\mathbf{I}/2 - \Xi \succ \mathbf{0}$, the convergence of the ADMM method can be guaranteed by the analysis in [25], we omit the details for brevity.

Algorithm 1 The ADMM Algorithm to (20)

1: **Initialization**: Set a feasible point $\left\{\mathbf{F}^1, \mathbf{Q}^1, \mathbf{P}^1\right\}$, and $m = 1$.
2: **repeat**
3: Optimize $\mathbf{F}^{m+1}$ by CVX.
4: Calculate $\mathbf{Q}^{m+1}$ by (27) or (32).
5: Calculate $\mathbf{P}^{m+1}$ by (22c).
6: $m \leftarrow m + 1$.
7: **until** the stopping criterion is met.
8: **Output** $\{\mathbf{F}^\star, \mathbf{Q}^\star, \mathbf{P}^\star\}$.

C. THE TRAJECTORY DESIGN

With given $\{\mathbf{W}, \mathbf{F}, \boldsymbol{\beta}\}$, the subproblem w.r.t. the trajectory $\mathbf{q}$ is formulated as:

$$\min_{\mathbf{q}} \sum_{n=1}^{N}\sum_{k=1}^{K}|\beta_k|^2\tilde{\sigma}_k^2\left(\|\mathbf{q} - \mathbf{q}_k\|^2\right) \tag{34a}$$

$$\text{s.t. } (1). \tag{34b}$$

It is known that (34) is a convex problem w.r.t. $\mathbf{q}$, which can be solved by the standard convex solver such as CVX [35], as the commonly used method in several literatures about trajectory design. However, in the work, we will propose a low complexity method to design the trajectory based on the ADMM method.

Specifically, the Lagrangian of (34) is given by

$$\begin{aligned}&\mathcal{L}\left(\mathbf{q},\mathbf{x},\mathbf{z},\boldsymbol{\lambda}_1,\boldsymbol{\lambda}_2\right)\\&=\sum_{n=1}^{N}\sum_{k=1}^{K}|\beta_k|^2\tilde{\sigma}_k^2\left(\|\mathbf{q}-\mathbf{q}_k\|^2\right)\\&\quad+\frac{\rho_1}{2}\|\mathbf{q}-\mathbf{x}+\boldsymbol{\lambda}_1\|^2+\frac{\rho_2}{2}\|\mathbf{D}\mathbf{q}-\mathbf{p}-\mathbf{z}+\boldsymbol{\lambda}_2\|^2,\end{aligned}\tag{35}$$

where $\mathbf{x}$ is the copy of the original trajectory, $\{\mathbf{z},\mathbf{p},\mathbf{D}\}$ are the slack variables to decouple (1), one can refer the trajectory optimization in page 6 of [36] for more details about $\{\mathbf{z},\mathbf{p},\mathbf{D}\}$. In addition, $\rho_1\geq 0$ and $\rho_2\geq 0$ are the penalty factors, while $\boldsymbol{\lambda}_1$ and $\boldsymbol{\lambda}_2$ are the scaled dual variables.

Then, the following iterative steps are applied to solve (35)

$$\mathbf{x}^{l+1}=\arg\min\mathcal{L}\left(\mathbf{q}^l,\mathbf{x}^l,\mathbf{z}^l,\boldsymbol{\lambda}_1,\boldsymbol{\lambda}_2\right),\tag{36a}$$

$$\mathbf{q}^{l+1}=\arg\min\mathcal{L}\left(\mathbf{q}^l,\mathbf{x}^{l+1},\mathbf{z}^l,\boldsymbol{\lambda}_1,\boldsymbol{\lambda}_2\right),\tag{36b}$$

$$\mathbf{z}^{l+1}=\underset{|\mathbf{z}_n|\leq S_{\max}}{\arg\min}\mathcal{L}\left(\mathbf{q}^{l+1},\mathbf{x}^{l+1},\mathbf{z}^l,\boldsymbol{\lambda}_1,\boldsymbol{\lambda}_2\right),\tag{36c}$$

$$\boldsymbol{\lambda}_1=\boldsymbol{\lambda}_1+\mathbf{q}-\mathbf{x},\tag{36d}$$

$$\boldsymbol{\lambda}_2=\boldsymbol{\lambda}_2+\mathbf{D}\mathbf{q}-\mathbf{p}-\mathbf{z},\tag{36e}$$

for $n=1,\ldots$ until certain stop criterion is meet [36].

The main advantage of the ADMM algorithm is that all the subproblems have closed-form solution. Specifically, the subproblem w.r.t. $\mathbf{x}$ is

$$\min_{\mathbf{x}}\sum_{n=1}^{N}\sum_{k=1}^{K}|\beta_k|^2\tilde{\sigma}_k^2\left(\|\mathbf{x}-\mathbf{q}_k\|^2\right)+\frac{\rho_1}{2}\|\mathbf{q}-\mathbf{x}+\boldsymbol{\lambda}_1\|^2,\tag{37}$$

via the first order condition, the optimal solution is

$$\begin{aligned}\mathbf{x}^{\star}[n]=&\left(2\sum_{k=1}^{K}|\beta_k[n]|^2\tilde{\sigma}_k^2+\rho_1\right)^{-1}\\&\times\left(\rho_1\mathbf{q}[n]-\rho_1\boldsymbol{\lambda}_1[n]+2\sum_{k=1}^{K}|\beta_k[n]|^2\tilde{\sigma}_k^2\mathbf{q}_k\right).\end{aligned}\tag{38}$$

Then, the subproblem w.r.t. $\mathbf{q}$ is

$$\frac{\rho_1}{2}\|\mathbf{q}-\mathbf{x}+\boldsymbol{\lambda}_1\|^2+\frac{\rho_2}{2}\|\mathbf{D}\mathbf{q}-\mathbf{p}-\mathbf{z}+\boldsymbol{\lambda}_2\|^2,\tag{39}$$

and the optimal solution is

$$\begin{aligned}\mathbf{q}^{\star}=&\left(\rho_1\mathbf{I}+\rho_2\mathbf{D}^T\mathbf{D}\right)^{-1}\\&\times\left(\rho_1\left(\mathbf{x}-\boldsymbol{\lambda}_1\right)+\rho_2\mathbf{D}^T\left(\mathbf{p}+\mathbf{z}-\boldsymbol{\lambda}_2\right)\right).\end{aligned}\tag{40}$$

Lastly, the subproblem w.r.t. $\mathbf{z}$ is

$$\|\mathbf{D}\mathbf{q}-\mathbf{p}-\mathbf{z}+\boldsymbol{\lambda}_2\|^2,\tag{41}$$

and the optimal solution is

$$\mathbf{z}_n^{\star}=\begin{cases}\mathcal{P}_{\mathcal{Z}}\left(\mathbf{q}[1]-\mathbf{q}_0+\boldsymbol{\lambda}_2[1]\right), & n=1,\\ \mathcal{P}_{\mathcal{Z}}\left(\mathbf{q}[n]-\mathbf{q}[n-1]+\boldsymbol{\lambda}_2[n]\right), & n=2,\ldots,N,\\ \mathcal{P}_{\mathcal{Z}}\left(\mathbf{q}_f-\mathbf{q}[N]+\boldsymbol{\lambda}_2[n]\right), & n=N+1,\end{cases}\tag{42}$$

where $\mathcal{P}_{\mathcal{Z}}(x)=\min\left\{\frac{S_{\max}}{|x|},1\right\}x$ denotes the projector associated with the linear space $\mathcal{Z}$.

To this end, the ADMM algorithm to obtain $\mathbf{q}$ is summarized in Algorithm 2.

Algorithm 2 The ADMM Algorithm to (34)

1: **Initialization**: Set a feasible point $\left\{\mathbf{x}^1,\mathbf{q}^1,\mathbf{z}^1\right\}$, and $m=1$.
2: **repeat**
3: Calculate $\mathbf{x}^m$ by (38).
4: Calculate $\mathbf{q}^m$ by (40).
5: Calculate $\mathbf{z}^m$ by (42).
6: $m\leftarrow m+1$.
7: **until** the stopping criterion is met.
8: **Output** $\left\{\mathbf{q}^{\star},\mathbf{x}^{\star},\mathbf{z}^{\star},\boldsymbol{\lambda}_1^{\star},\boldsymbol{\lambda}_2^{\star}\right\}$.

Finally, the entail procedure for (8) is summarized in Algorithm 3, where $\left\{\mathbf{w}_k^l,\mathbf{F}^l,\mathbf{q}^l\right\}$ and WSR^l are the optimal solution and optimal value of (8) in the l-th iteration, respectively. In addition, ϵ denotes the stopping criterion, namely the tolerance.

Algorithm 3 The Lagrangian Method to (8)

1: **Initialization**: Set P_s, $\mathbf{h}_k$, the initial $\left\{\mathbf{w}_k^1,\mathbf{F}^1,\mathbf{q}^1\right\}$, and $l=1$.
2: **repeat**
3: Update $\mathbf{w}_k^l$ by solving (16).
4: Update $\mathbf{F}^l$ by solving (19) with the ADMM method.
5: Update $\mathbf{q}^l$ by solving (34).
6: Update β_k^l by solving (15).
7: Update $\alpha_k^l=\dfrac{\left|\mathbf{h}_k^H\mathbf{F}\mathbf{w}_k\right|^2}{\sum\limits_{i=1,i\neq k}^{K}\left|\mathbf{h}_k^H\mathbf{F}\mathbf{w}_i\right|^2+\tilde{\sigma}_k^2\left(H^2+\|\mathbf{q}-\mathbf{q}_k\|^2\right)}$.
8: $l\leftarrow l+1$.
9: **until** $WSR^l-WSR^{l-1}\leq\varepsilon$.
10: **Output** $\left\{\mathbf{w}_k^{\star},\mathbf{F}^{\star},\mathbf{q}^{\star}\right\}$.

D. OPTIMALITY AND COMPUTATIONAL COMPLEXITY ANALYSIS

In this subsection, we analyze the optimality and computational complexity of the proposed AO method. Firstly, the optimality and convergence of each subproblem can be guaranteed by the conclusion in related works. Specifically, the optimality and convergence of the Lagrangian dual transform is analyzed in [31]. Also, the optimality and convergence of the digital BF method is analyzed in [32]. While the optimality and convergence of the ADMM method to design the analog BF is given in [25]. Besides, the optimality and convergence of the ADMM method to design the trajectory is given in [36]. Then, based on the convergence of each subproblem and the feature of AO, the convergence of the AO method can be guaranteed [34]. However, since the original problem (8) is not convex w.r.t. all these variables, thus only suboptimal solution can be obtained by the AO method [30].

Then, we focus on the computational complexity of the proposed AO method, which is mainly determined by the complexity of each subproblem. Specifically, for the optimization of $\mathbf{w}_k$, in each step of the bisection search method, the main complexity is to calculate $\mathbf{w}_k$ in (17), which is given by $\mathcal{O}\left(NKN_t^3N_{RF}^3\right)$ [31]. The required number of iterations for Algorithm 1 to converge is $\log_2\left(\frac{\lambda_u-\lambda_l}{\varepsilon}\right)$, where ε denotes the accuracy tolerance, λ_u and λ_l are the bounds of λ. Hence, the total complexity of Algorithm 1 is $\mathcal{O}\left(\log_2\left(\frac{\lambda_u-\lambda_l}{\varepsilon}\right)NKN_t^3N_{RF}^3\right)$ [32].

Then, for the ADMM algorithm to update $\mathbf{F}$, according to [25], the complexity is $\mathcal{O}\left(T_FNN_t^3N_{RF}^3\right)$, where T_F denotes the number of iterations required for convergence. As for the optimization of trajectory $\mathbf{q}$, according to [36], the complexity is given by $\mathcal{O}\left(T_qN^2\right)$, where T_q denotes the number of iterations required for convergence. However, when CVX is utilized to obtain $\mathbf{q}$, according to [35] and [36], the complexity is given by $O\left(N^{7/2}\right)$, which will be higher than the ADMM method, especially for large N.

From the above analysis, the overall complexity of the proposed AO method can be estimated by [30]

$$C_{\mathrm{AO}} = O\left(\max\left\{\log_2\left(\frac{\lambda_u-\lambda_l}{\varepsilon}\right)NKN_t^3N_{RF}^3\ ,\ T_FNN_t^3N_{RF}^3, T_qN^2\right\}\right). \quad (43)$$

From this analysis, we can see that the proposed algorithm obtain polynomial time complexity, which is beneficial for practical implementation.

IV. SIMULATION RESULTS

In this section, we provide some Monte-Carlo (MC) simulations to testify the performance of the proposed scheme. Unless specified, the simulation setting are set as: $T = 80s$, $\delta_T = 0.5s$, $\hat{P} = 4\bar{P}$ with $\bar{P} = 20dBm$, while the noise power is $\sigma_k^2 = -80dBm, \forall k \in \mathcal{K}$, $N_t = 8$, $N_{RF} = 4$, $V_{\max} = 10m/s$, and $H = 100m$. The horizontal coordinates of the initial and final locations of the UAV are set as $\mathbf{q}_0 = [100, 200]^T$ and $\mathbf{q}_F = [100, -200]^T$, respectively. Besides, there exist 4 users, which are located at $[50, 20]^T$, $[50, -20]^T$, $[150, 20]^T$, and $[150, -20]^T$, respectively.

A. CONVERGENCE BEHAVIOUR

Firstly, we investigate the convergence behaviour of the proposed AO algorithm. Fig. 4 shows the convergence behaviour of the inner ADMM algorithm with different N_t and N_{RF}. From Fig. 4, we can see that the WSR increases with the number of iterations, and finally converges. Moreover, higher WSR can be achieved by using larger N_t or N_{RF}. However, larger N_t or N_{RF} leads to slower convergence, since more variables need to be optimized.

Now, we investigate the convergence behaviour of the outer AO algorithm. Fig. 5 shows the WSR versus the number of iterations with different N_t and N_{RF}. It can be seen from Fig. 5 that, for different values of N_t and N_{RF}, the AO algorithm always converge within 20 iterations, which confirms the practicality of the proposed design.

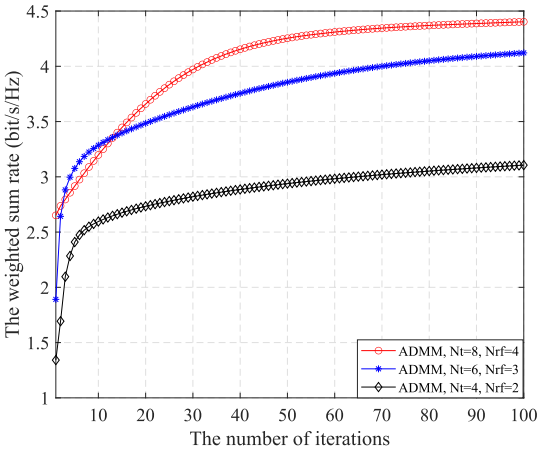

FIGURE 4. Convergence behaviour of the inner layer iteration.

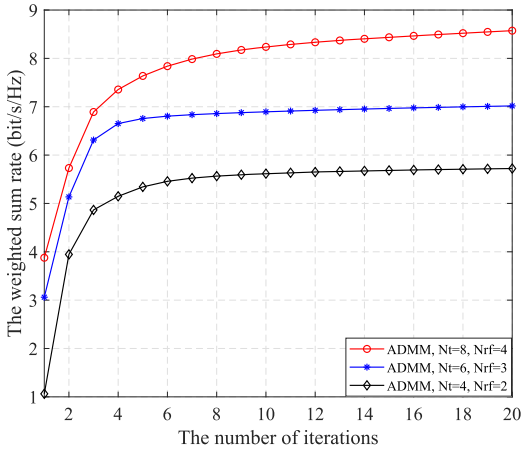

FIGURE 5. Convergence behaviour of the outer layer iteration.

B. PERFORMANCE EVALUATION

In this subsection, we investigate the WSR performance versus the main system parameters. In addition, we compare the proposed method with the following benchmark schemes: 1) the fully digital BF method, i.e., the BF is obtained by the fully digital method, which can be seen as the upper bound of the hybrid BF method; 2) the fully-connected BF with the CVX based trajectory design, which is a comparison to the ADMM based trajectory design; 3) the no trajectory design method, i.e., the UAV fly directly from the initial location to the final location. This comparison can show the effect of the trajectory design in UAV communication system; 4) the random hybrid BF method, i.e., choose the BF vector randomly. This comparison can show the effect of the proposed BF method. These methods are labelled as "Fully-connected case", "Sub-connected case", "Fully digital BF method", "CVX based trajectory design", "No trajectory design method", and "Random BF method", respectively.

Firstly, we show the WSRs of these schemes versus the transmit power budget of the UAV $\bar{P}$. It can be seen from

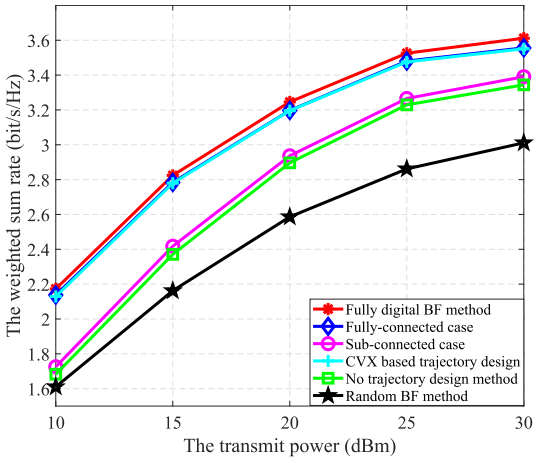

FIGURE 6. The weighted sum rate versus the transmit power budget.

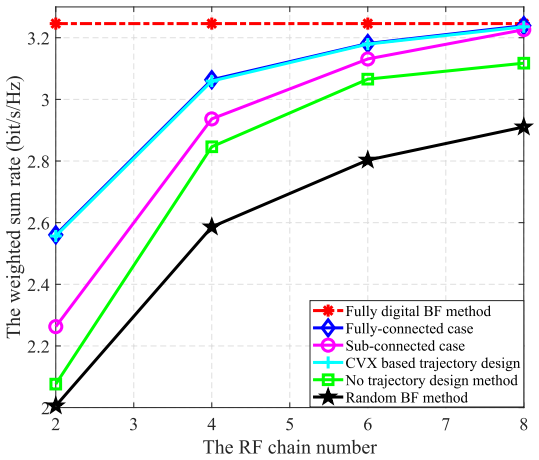

FIGURE 7. The weighted sum rate versus the UAV RF chain number.

Fig. 6 that, with the increase of $\bar{P}$, the WSRs increase for all these methods, while the proposed method outperforms the random BF method and the no trajectory design method, which shows the importance of joint BF and trajectory design. In addition, the ADMM-based trajectory design obtains a nearly performance with the CVX based trajectory design, which suggests the effectiveness of the ADMM method, while the fully-connected structure outperforms the sub-connected structure, and the performance gap between the proposed method and the fully digital BF method is small, which will be further confirmed by the following simulations.

Then, in Fig. 7, we show the WSRs of these schemes versus the RF chain number N_{RF}. From this figure, we can see that more N_{RF} leads to higher WSR. In addition, with the increase of N_{RF}, the performance gap between the proposed hybrid BF and the fully digital BF method tends to small, when $N_{RF} = N_t$, the proposed method can obtain similar performance with the fully digital BF method, which shows the superiority of the proposed design. Besides, with the increase of N_{RF}, the sub-connected structure can achieve nearly performance to the fully-connected structure, which is consistent with the results in related literatures such as [21].

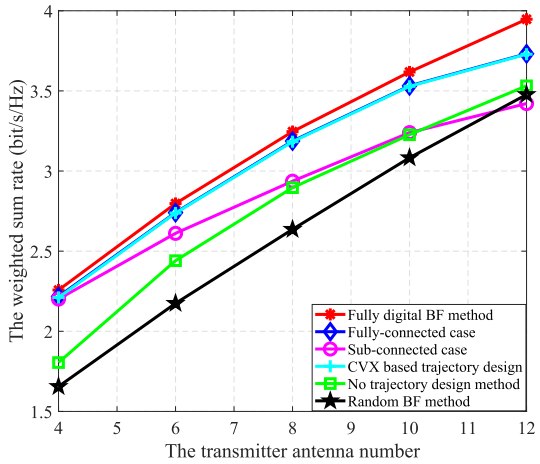

FIGURE 8. The weighted sum rate versus the UAV antenna number.

This result suggests the effectiveness for the ADMM method in the sub-connected structure.

Lastly, in Fig. 8, we show the WSRs of these schemes versus the UAV antenna number N_r. From this figure, we can see that more N_r leads to higher WSR, since higher spatial degree of freedom can be achieved. In addition, with the increase of N_r, the performance gap between the fully digital BF method and the hybrid BF method tends to larger, since with the increase of N_r, the dimensions of the variables in the fully digital BF method will be more greater than the hybrid BF method, at the expenses of higher hardware cost.

V. CONCLUSION

This work has studied the transmission design in multi antenna UAV-enabled downlink multiuser network. Specifically, we aimed to maximize the WSR by jointly designing the hybrid BF and flight trajectory of the UAV. To handle the formulated non-convex problem, we proposed an AO method which linearize the objective by a newly Lagrangian dual transform, where each subproblem can be solved with low complexity. Simulation results verified the performance the proposed method. In our future work, to further reduce the cost and energy consumption of the UAV, another alternative technique such as the intelligent reflecting surface to achieve high beamforming gain will be investigated.

REFERENCES

[1] Y. Kawamoto, H. Nishiyama, N. Kato, F. Ono, and R. Miura, "Toward future unmanned aerial vehicle networks: Architecture, resource allocation and field experiments," *IEEE Wireless Commun.*, vol. 26, no. 1, pp. 94–99, Feb. 2019.

[2] J. Xu, Y. Zeng, and R. Zhang, "UAV-enabled wireless power transfer: Trajectory design and energy optimization," *IEEE Trans. Wireless Commun.*, vol. 17, no. 8, pp. 5092–5106, Aug. 2018.

[3] H. Tang, Q. Wu, and B. Li, "An efficient solution for joint power and trajectory optimization in UAV-enabled wireless network," *IEEE Access*, vol. 7, pp. 59625–59640, Mar. 2019.

[4] G. Zhang, Q. Wu, M. Cui, and R. Zhang, "Securing UAV communications via joint trajectory and power control," *IEEE Trans. Wireless Commun.*, vol. 18, no. 2, pp. 1376–1389, Feb. 2019.

[5] Q. Wu, Y. Zeng, and R. Zhang, "Joint trajectory and communication design for multi-UAV enabled wireless networks," *IEEE Trans. Wireless Commun.*, vol. 17, no. 3, pp. 2109–2121, Mar. 2018.

[6] I. Valiulahi and C. Masouros, "Multi-UAV deployment for throughput maximization in the presence of co-channel interference," *IEEE Internet Things J.*, vol. 8, no. 5, pp. 3605–3618, Mar. 2021.
[7] C. Shen, T.-H. Chang, J. Gong, Y. Zeng, and R. Zhang, "Multi-UAV interference coordination via joint trajectory and power control," *IEEE Trans. Signal Process.*, vol. 68, pp. 843–858, May 2020.
[8] J. Ji, K. Zhu, D. Niyato, and R. Wang, "Joint cache placement, flight trajectory, and transmission power optimization for multi-UAV assisted wireless networks," *IEEE Trans. Wireless Commun.*, vol. 19, no. 8, pp. 5389–5402, Aug. 2020.
[9] Y. Sun, D. Xu, D. W. K. Ng, L. Dai, and R. Schober, "Optimal 3D-trajectory design and resource allocation for solar-powered UAV communication systems," *IEEE Trans. Commun.*, vol. 67, no. 6, pp. 4281–4298, Jun. 2019.
[10] F. Zeng, Z. Hu, Z. Xiao, H. Jiang, S. Zhou, W. Liu, and D. Liu, "Resource allocation and trajectory optimization for QoE provisioning in energy-efficient UAV-enabled wireless networks," *IEEE Trans. Veh. Technol.*, vol. 69, no. 7, pp. 7634–7647, Jul. 2020.
[11] M. Hua, Y. Wang, Q. Wu, H. Dai, Y. Huang, and L. Yang, "Energy-efficient cooperative secure transmission in multi-UAV-enabled wireless networks," *IEEE Trans. Veh. Technol.*, vol. 68, no. 8, pp. 7761–7775, Aug. 2019.
[12] X. Zhou, Q. Wu, S. Yan, F. Shu, and J. Li, "UAV-enabled secure communications: Joint trajectory and transmit power optimization," *IEEE Trans. Veh. Technol.*, vol. 68, no. 4, pp. 4069–4073, Apr. 2019.
[13] Y. Zhou, F. Zhou, H. Zhou, D. W. K. Ng, and R. Q. Hu, "Robust trajectory and transmit power optimization for secure UAV-enabled cognitive radio networks," *IEEE Trans. Commun.*, vol. 68, no. 7, pp. 4022–4034, Jul. 2020.
[14] T. Lin, J. Cong, Y. Zhu, J. Zhang, and K. Ben Letaief, "Hybrid beamforming for millimeter wave systems using the MMSE criterion," *IEEE Trans. Commun.*, vol. 67, no. 5, pp. 3693–3708, May 2019.
[15] D. Xu, Y. Sun, D. W. K. Ng, and R. Schober, "Multiuser MISO UAV communications in uncertain environments with no-fly zones: Robust trajectory and resource allocation design," *IEEE Trans. Commun.*, vol. 68, no. 5, pp. 3153–3172, May 2020.
[16] Y. Cai, Z. Wei, R. Li, D. W. K. Ng, and J. Yuan, "Joint trajectory and resource allocation design for energy-efficient secure UAV communication systems," *IEEE Trans. Commun.*, vol. 68, no. 7, pp. 4536–4553, Jul. 2020.
[17] H. Wu, Y. Wen, J. Zhang, Z. Wei, N. Zhang, and X. Tao, "Energy-efficient and secure air-to-ground communication with jittering UAV," *IEEE Trans. Veh. Technol.*, vol. 69, no. 4, pp. 3954–3967, Apr. 2020.
[18] L. Dai, B. Wang, M. Peng, and S. Chen, "Hybrid precoding-based millimeter-wave massive MIMO-NOMA with simultaneous wireless information and power transfer," *IEEE J. Sel. Areas Commun.*, vol. 37, no. 1, pp. 131–141, Jan. 2019.
[19] C. Xing, X. Zhao, W. Xu, X. Dong, and G. Y. Li, "A framework on hybrid MIMO transceiver design based on matrix-monotonic optimization," *IEEE Trans. Signal Process.*, vol. 67, no. 13, pp. 3531–3546, Jul. 2019.
[20] J. Jin, Y. R. Zheng, W. Chen, and C. Xiao, "Hybrid precoding for millimeter wave MIMO systems: A matrix factorization approach," *IEEE Trans. Wireless Commun.*, vol. 17, no. 5, pp. 3327–3339, May 2018.
[21] A. Arora, C. G. Tsinos, B. S. M. R. Rao, S. Chatzinotas, and B. Ottersten, "Hybrid transceivers design for large-scale antenna arrays using majorization-minimization algorithms," *IEEE Trans. Signal Process.*, vol. 68, pp. 701–714, 2020.
[22] H. Ruan, P. Xiao, L. Xiao, and J. R. Kelly, "Joint iterative optimization-based low-complexity adaptive hybrid beamforming for massive MU-MIMO systems," *IEEE Trans. Commun.*, vol. 69, no. 3, pp. 1707–1722, Mar. 2021, doi: 10.1109/TCOMM.2021.3053021.
[23] J. Xu, W. Xu, D. W. K. Ng, and A. L. Swindlehurst, "Secure communication for spatially sparse millimeter-wave massive MIMO channels via hybrid precoding," *IEEE Trans. Commun.*, vol. 68, no. 2, pp. 887–901, Feb. 2020.
[24] W. Ma, C. Qi, Z. Zhang, and J. Cheng, "Sparse channel estimation and hybrid precoding using deep learning for millimeter wave massive MIMO," *IEEE Trans. Commun.*, vol. 68, no. 5, pp. 2838–2849, May 2020.
[25] Q. Li, C. Li, and J. Lin, "Constant modulus secure beamforming for multicast massive MIMO wiretap channels," *IEEE Trans. Inf. Forensics Security*, vol. 15, pp. 264–275, Jul. 2020.
[26] B. Li, Z. Fei, and Y. Zhang, "UAV communications for 5G and beyond: Recent advances and future trends," *IEEE Internet Things J.*, vol. 6, no. 2, pp. 2241–2263, Apr. 2019.
[27] *Study on Enhanced LTE Support for Aerial Vehicles*, document TR 36.777, V15.0.0, 3GPP, Dec. 2017.
[28] M. Mozaffari, W. Saad, M. Bennis, Y.-H. Nam, and M. Debbah, "A tutorial on UAVs for wireless networks: Applications, challenges, and open problems," *IEEE Commun. Surveys Tuts.*, vol. 21, no. 3, pp. 2334–2360, 3rd Quart., 2019.
[29] C. G. Tsinos, S. Maleki, S. Chatzinotas, and B. Ottersten, "On the energy-efficiency of hybrid analog–digital transceivers for single- and multi-carrier large antenna array systems," *IEEE J. Sel. Areas Commun.*, vol. 35, no. 9, pp. 1980–1995, Sep. 2017.
[30] S. Boyd and L. Vandenberghe, *Convex Optimization*. Cambridge, U.K.: Cambridge Univ. Press, 2004.
[31] K. Shen and W. Yu, "Fractional programming for communication systems—Part I: Power control and beamforming," *IEEE Trans. Signal Process.*, vol. 66, no. 10, pp. 2616–2630, May 2018.
[32] K. Shen and W. Yu, "Fractional programming for communication systems—Part II: Uplink scheduling via matching," *IEEE Trans. Signal Process.*, vol. 66, no. 10, pp. 2631–2644, May 2018.
[33] J. Gorski, F. Pfeuffer, and K. Klamroth, "Biconvex sets and optimization with biconvex functions: A survey and extensions," *Math. Methods Operations Res.*, vol. 66, no. 3, pp. 373–407, Nov. 2007.
[34] X. Yu, J.-C. Shen, J. Zhang, and K. B. Letaief, "Alternating minimization algorithms for hybrid precoding in millimeter wave MIMO systems," *IEEE J. Sel. Topics Signal Process.*, vol. 10, no. 3, pp. 485–500, Apr. 2016.
[35] M. Grant and S. Boyd. (Sep. 2012). *CVX: MATLAB Software for Disciplined Convex Programming, Version 2.0 Beta*. [Online]. Available: http://cvxr.com/cvx
[36] Y. Gao, H. Tang, B. Li, and X. Yuan, "Joint trajectory and power design for UAV-enabled secure communications with no-fly zone constraints," *IEEE Access*, vol. 7, pp. 44459–44470, Apr. 2019.

FENG ZHOU received the B.S. and M.S. degrees from Southeast University, Nanjing, China, in 2004 and 2012, respectively. He is currently pursuing the Ph.D. degree with the Army Engineering University of PLA.

Since 2017, he has been an Associate Professor with the College of Information Engineering, Yancheng Institute of Technology, Yancheng, China. His research interests include cooperative communication, physical layer security, and UAV communication.

RUGANG WANG received the B.S. degree from the Wuhan University of Technology, Wuhan, China, in 1999, the M.S. degree from Jinan University, Guangzhou, China, in 2007, and the Ph.D. degree from Nanjing University, Nanjing, China, in 2012.

Since 2012, he has been an Associate Professor with the College of Information Engineering, Yancheng Institute of Technology, Yancheng, China. His research interests include the beamforming technique, UAV communication, and cooperative communication.